Steinberg et al., http://www.jcb.org/cgi/content/full/jcb.201111121/DC1

Figure S1. **Quantification of SNX17 suppression by individual oligos and resultant effects on loss of Itgα5β1 as determined by SILAC-based proteomics, Western blot analysis, and a cell-based recycling assay.** (A) Western blot showing RNAi efficiency in SILAC-labeled cells. (B) The table lists all integrins detected in the SILAC experiment with the respective ratios when quantification was possible. (C) Quantitative RT-PCR analysis of mRNA levels of the indicated genes in SNX17-depleted HeLa cells. Error bars represent the standard deviation from two experiments performed in triplicates (*, $P < 0.05$). (D) Fluorescent Western blot of Itgα5β1 in cells depleted with four different siRNAs against SNX17. (E) Quantification of residual SNX17 in HeLa cells treated with the indicated oligos. Error bars represent the standard deviation of four experiments. (F) Plot of residual SNX17 abundance against levels of mature Itgβ1 and total α5 in the respective cells. The line indicates the trend. (G) Antibody-based Itgβ1 recycling assay with an antibody against active (TS2/16) Itgβ1. The images show recycling of the antibody back to the surface (nonpermeabilized) and antibody remaining within the cells (permeabilized) after a 30-min chase period in control and SNX17-depleted cells. Bars, 10 µm. IB, immunoblot; KD, knockdown.

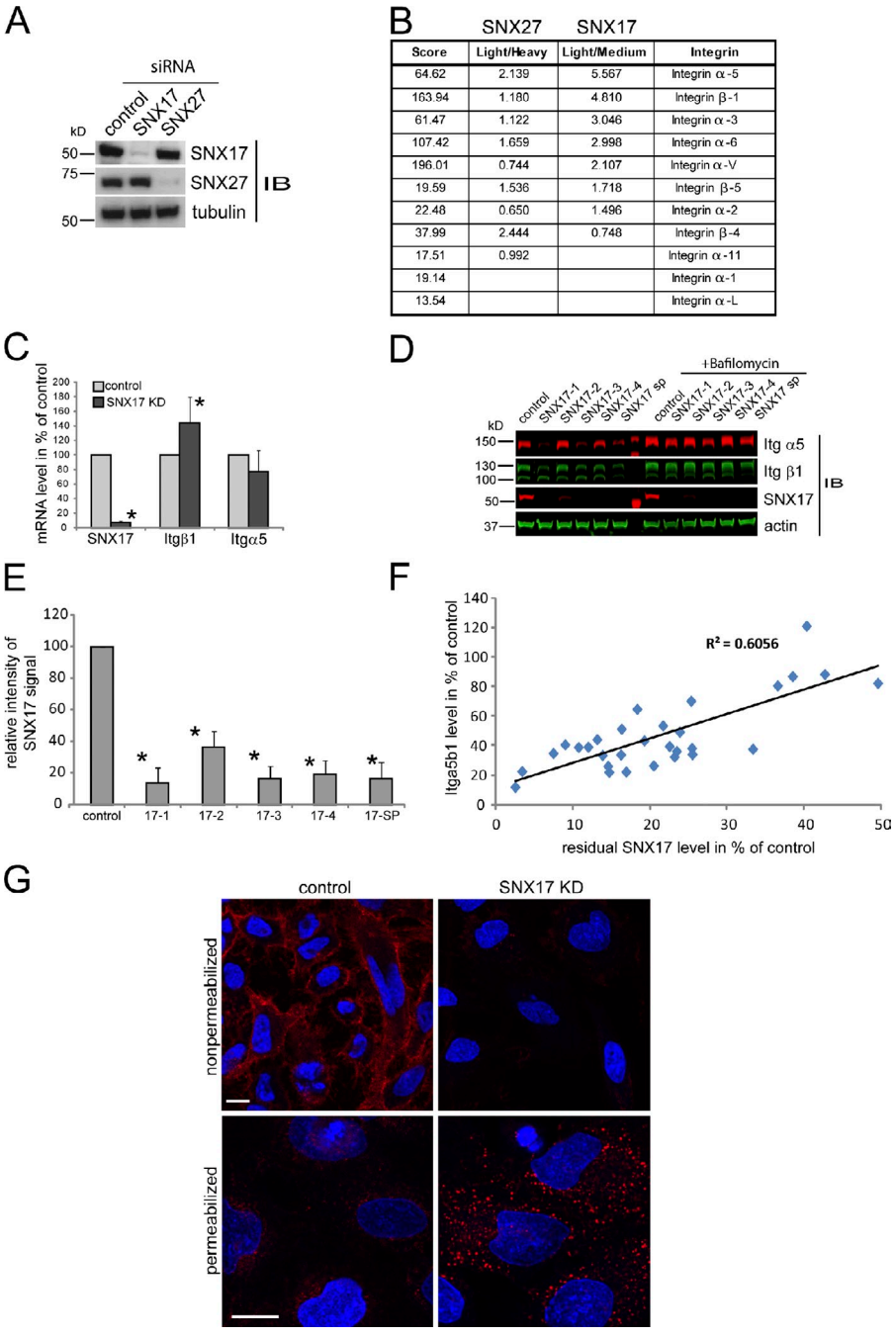

Score	Light/Heavy	Light/Medium	Integrin
64.62	2.139	5.567	Integrin α-5
163.94	1.180	4.810	Integrin β-1
61.47	1.122	3.046	Integrin α-3
107.42	1.659	2.998	Integrin α-6
196.01	0.744	2.107	Integrin α-V
19.59	1.536	1.718	Integrin β-5
22.48	0.650	1.496	Integrin α-2
37.99	2.444	0.748	Integrin β-4
17.51	0.992		Integrin α-11
19.14			Integrin α-1
13.54			Integrin α-L

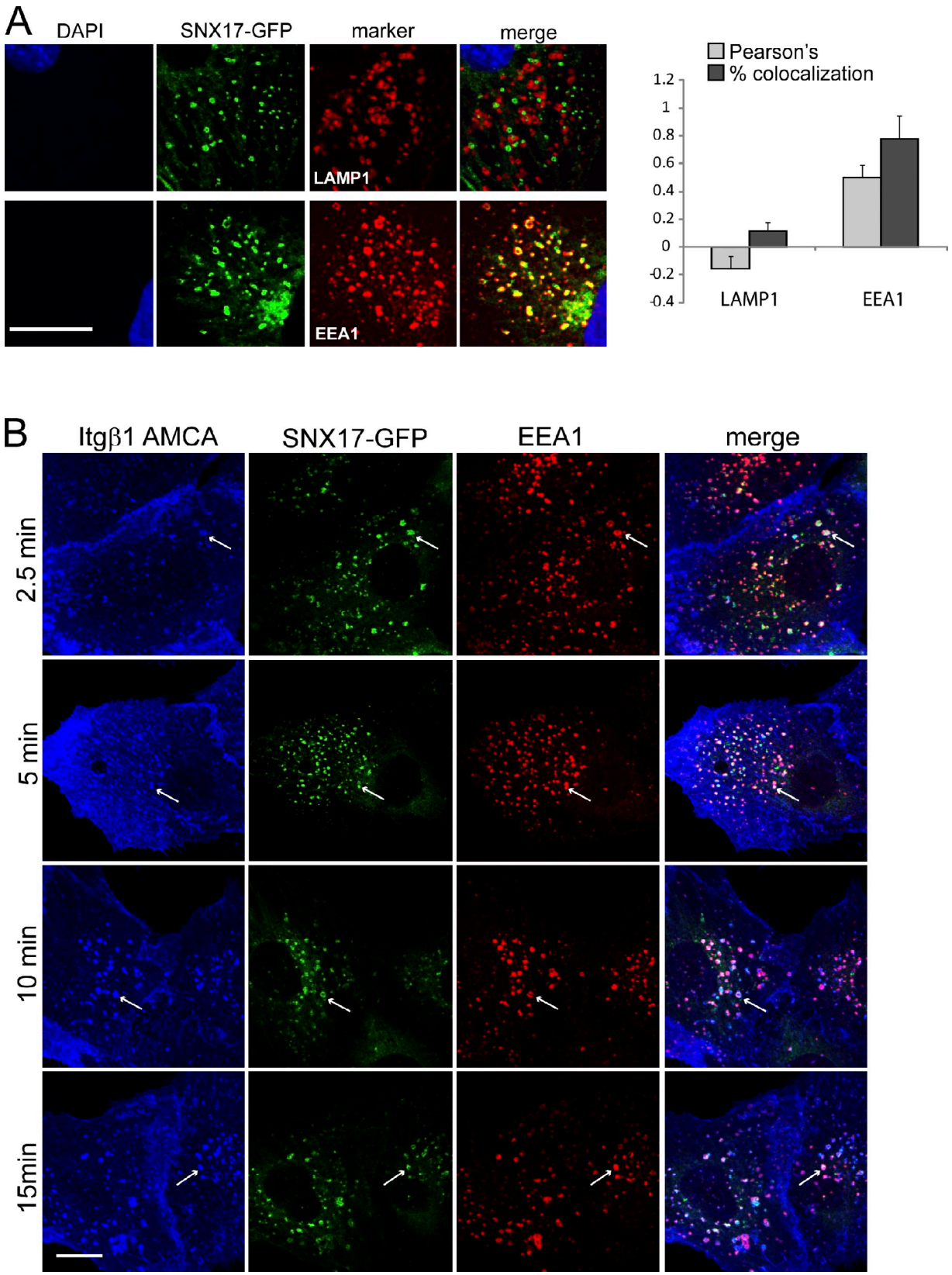

Figure S2. **Colocalization analysis of SNX17-GFP with endogenous EEA1 and LAMP1.** (A) The graph represents quantitative data from 12 images for each marker. The error bars indicate the standard deviation. (B) Colocalization analysis of internalized antibody against active Itgβ1, SNX17-GFP, and endogenous EEA1 after the indicated internalization periods. The arrows indicate spots of colocalization. Bars, 10 µm. AMCA, amino-methyl-coumarin-acetate.

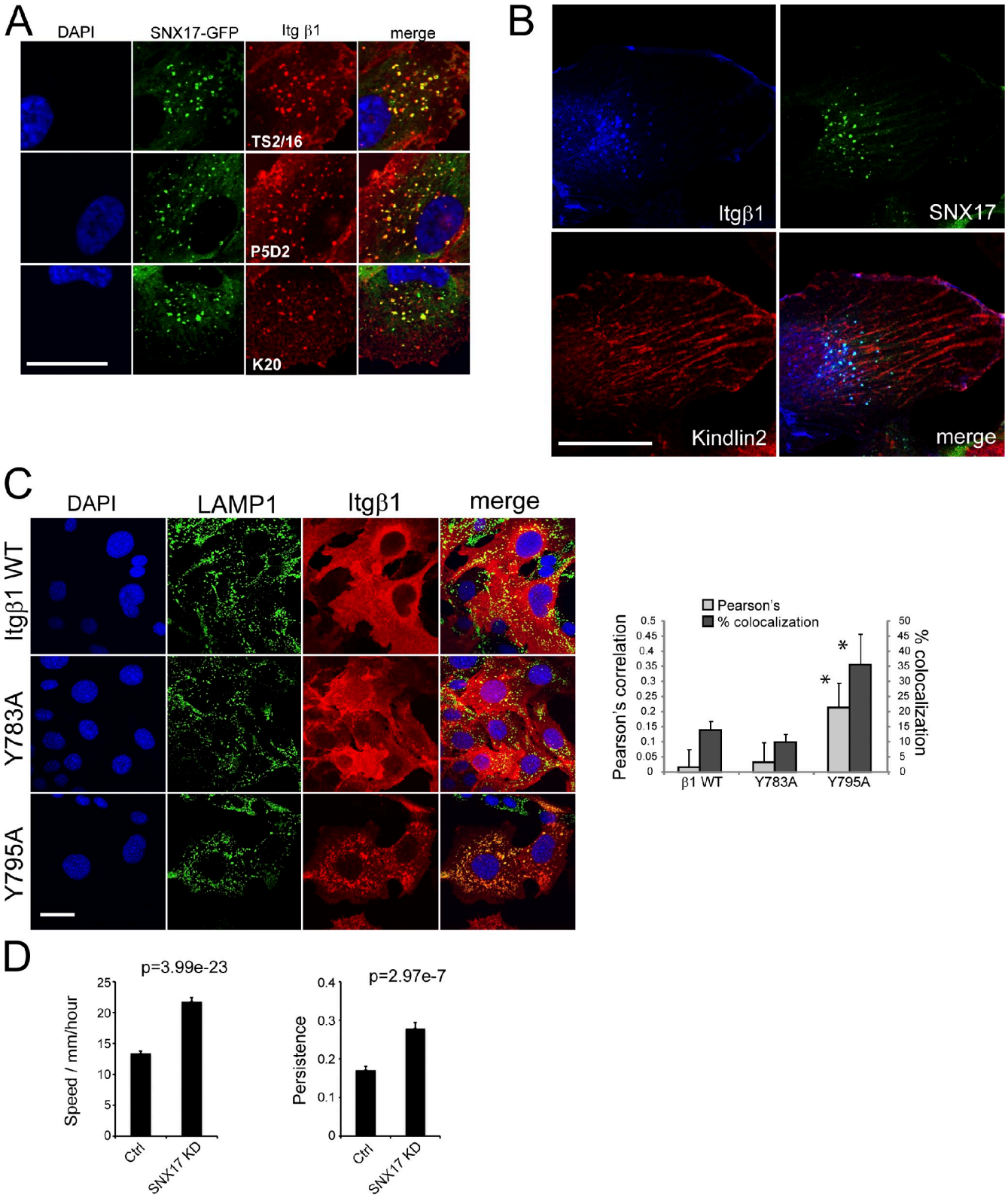

Figure S3. **Internalization of active versus inactive Itgβ1 into SNX17-GFP endosomes and the importance of the Y795A for retrieval from the lysosomal compartment.** (A) Colocalization of internalized antibody against active (TS2/16), inactive (P5D2), and total (K20) Itgβ1 and SNX17-GFP after 30 min of internalization. (B) Colocalization of internalized antibody against active Itgβ1, SNX17-GFP, and endogenous Kindlin-2. (C) Colocalization analysis of active human Itgβ1 virally expressed in Itgβ1$^{-/-}$ MEFs and endogenous LAMP1. The graph represents an analysis of 12 images for each group. The error bars indicate the standard deviation (*, P < 0.05). (D) Migration speed and persistence in control and SNX17-depleted HeLa cells in a 3D matrix. Bars, 20 µm. Ctrl, control; KD, knockdown; WT, wild type.

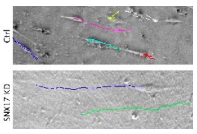

Video 1. **Fibroblasts transfected with control or SNX17-targeted siRNA migrating through a fibrillar cell-derived matrix.** Images were analyzed by time-lapse microscopy using a microscope (AS MDW). Frames were taken every 10 min for 10 h. The colored lines indicate the tracking of the migratory path of the cells. KD, knockdown; Ctrl, control.